

MAR 13 1998

B Physics at CDF

A. B. Wicklund

R

High Energy Physics Division
Argonne National Laboratory
Argonne, IL. 60439

Abstract. The CDF experiment at the Fermilab Tevatron has proven to be well suited for precision studies of b physics. Thanks to the excellent performance of the Tevatron Collider and the detector, CDF has accumulated very large data samples and roughly a decade of experience with b physics in $p\bar{p}$ collisions. With the much higher luminosities expected for the Main Injector era, the next decade promises to be an even more fruitful period for CDF. Here we offer a brief overview of issues in hadron-collider b physics and a summary of CDF's accomplishments and future plans.

OVERVIEW

Although b physics was not mentioned in the original 1981 CDF technical design report [1,2], several features were incorporated in the CDF design that made precision b physics possible. These included: a large solenoidal magnetic tracking volume; a well segmented electron/photon calorimeter outside of the tracking region; and a relatively thin muon filter that allowed muon detection down to ~ 1.5 GeV/ c transverse momentum (p_T). While not intended for b physics, these detector capabilities allowed CDF to study basic features of b production in the first official physics run (so-called "Run 0", 1988-1989, 4 pb^{-1}), and to develop strategies for a more sophisticated program of b physics in the second physics run ("Run I", 1992-1996, 120 pb^{-1}), using a silicon vertex detector [3]. In turn, the experience gained from Run I now provides a baseline for planning the CDF b physics program in the Main Injector era ("Run II" and beyond) [4], including detector upgrades that will significantly expand on the present CDF capabilities.

The main motivation for pursuing b physics at hadron colliders is well known. The production cross sections measured at CDF at $\sqrt{s} = 1.8$ TeV imply total event yields of $10^{11} B\bar{B}$ pairs per fb^{-1} integrated luminosity, much higher than the yields expected for e^+e^- B-factories. This rate advantage is significant because once product branching ratios are taken into account,

* Work supported in part by the U.S. Department of Energy,
Division of High Energy Physics, Contract W-31-109-ENG-38.

The submitted manuscript has been authored by a contractor of the U.S. Government under contract No. W-31-109-ENG-38. Accordingly, the U.S. Government retains a nonexclusive, royalty-free license to publish or reproduce the published form of this contribution, or allow others to do so, for U.S. Government purposes.

ANL-HEP-CP-98-01
Fermilab Library
0 1160 0061221 2

almost all interesting B-decay modes are quite rare. For example, for the “ $\sin 2\beta$ ” mode, $B^0 \rightarrow \psi K_S$, $\psi \rightarrow \mu^+ \mu^-$, $K_S \rightarrow \pi^- \pi^+$, the combined branching ratio is 1.7×10^{-5} , and the production yields would be 1.4×10^6 events for 1 fb^{-1} at the Tevatron, compared with 500 events for 30 fb^{-1} at BABAR (nominal BABAR year). Even though trigger and event selection cuts on p_T and η reduce the geometrical efficiency at CDF to around 1% for this mode, the potential advantage is still rather large.

In addition to high rates, the Tevatron offers other features that are worth noting. First, $p\bar{p}$ is a CP -symmetric initial state, and so we expect equal rates for B and \bar{B} hadrons, at least in the central region. Second, the p_T spectrum for B hadrons scales like the B mass and is significantly harder than that for light hadrons. As a result, the B hadrons are Lorentz-boosted at all rapidities, including the central region where the production rate is highest; at $y=0$, the average $p_T(B)$ is around $3.5 \text{ GeV}/c$. Thus, with p_T cuts on the B decays, one can take advantage of the long B lifetime to identify B decays and to exploit the time dependence of mixing and CP violation signatures. Third, the hard $p_T(B)$ spectrum is also a useful tool in improving signal to background; whereas $B\bar{B}$ production makes up $\sim 0.2\%$ of the $p\bar{p}$ inelastic cross section, at high p_T the ratio of b jet to inclusive jet production is measured to be around 2%. Finally, the Tevatron (like LEP) produces all species of b hadrons, including B_s , Λ_b , Ξ_b , B_c , and B^* and B^{**} excitations; in this respect, b physics at the Tevatron complements that at the $\Upsilon(4S)$ B factories.

In order to take advantage of the potentially high yields at the Tevatron, efficient trigger schemes are needed. For Runs 0 and I, CDF relied on single and dilepton triggers to collect very large samples of semileptonic and J/ψ decays, with typical trigger thresholds at $p_T \sim 8 \text{ GeV}/c$ (single leptons) and at $p_T \sim 2 \text{ GeV}/c$ (dileptons). From silicon vertex-based analyses, the inclusive J/ψ sample has a B fraction of $\sim 20\%$, the remainder coming from prompt sources. Similarly, the inclusive lepton samples are found to be typically 40% from B decays, the remainder coming from $c\bar{c}$ production or fake leptons. Silicon vertex cuts can be used to further improve the B sample purities, but to start with, the signal to background in these samples is comparable to the b fractions that are produced in e^+e^- collisions at the $\Upsilon(4S)$ or the Z^0 poles ($\sim 20\%$).

Combining the high purity and large yields for these lepton trigger samples, the CDF Run I data provide the largest single sample of exclusive decays for J/ψ modes, ~ 1800 total events in $B \rightarrow \psi K_S$, ψK^+ , ψK^{*0} , $\psi \phi$, and $\psi \Lambda$. CDF also has the largest single sample of quasi-exclusive semi-leptonic decays, $\sim 10,000$ total events in the modes $B \rightarrow l^+ \nu D^0$, D^+ , D^{*+} , D_s , and Λ_c . Figure 1 shows examples of the $B^0 \rightarrow \psi K_S$ and ψK^{*0} and $B^+ \rightarrow \psi K^+$ signals from Run I. Figure 2 shows reconstructed charm peaks from semileptonic B^0 and B^+ decays. These correspond to total samples of order 10^5 $B \rightarrow J/\psi X$ and 10^6 $B \rightarrow l^+ \nu X$ inclusive events. For comparison, typical $B^0 \rightarrow \psi K_S$ yields at LEP are ~ 8 events per 3.6 million Z^0 decays [5], and at CLEO ~ 46 events

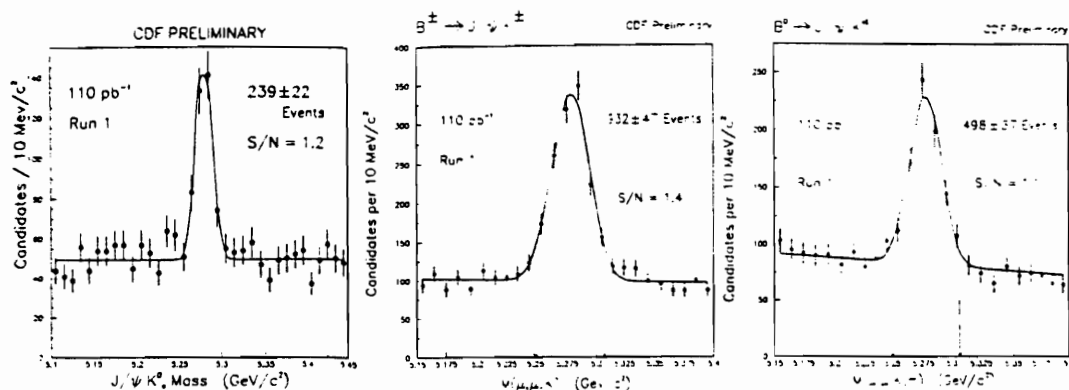


FIGURE 1. (left to right) ψK_S , ψK^+ , and ψK^0 mass peaks from CDF Run I.

per 3.1 fb^{-1} integrated luminosity [6]. Thus, for modes where CDF can exploit an efficient trigger, it is demonstrably possible to take advantage of the very large b production cross section in the central region.

While lepton and J/ψ triggers open up a broad palette of b physics, there are at least two further challenges that are not *easily* met at a hadron collider. The first is flavor tagging—identifying the flavor of a neutral B hadron at birth—needed for mixing and CP violation studies. This can be done by identifying the associated b jet in a $b\bar{b}$ final state, or by measuring the charge of the parent \bar{b} jet that produced the B^0 or B_s (“self-tagging” or “same-side tagging”). These place demands on the rapidity coverage for tracking and particle identification and on the ability to reject particles from associated gluon jets or underlying event debris. CDF has used both tagging methods to make competitive measurements of $B^0 - \bar{B}^0$ time-dependent mixing. Using the experience gained in Run I, CDF will improve the tagging efficiency in Run II by extending the tracking coverage in η , improving both muon and electron coverage, and possibly adding kaon identification by time-of-flight.

The second challenge is to trigger on all-hadronic B decays, such as $B^0 \rightarrow \pi^+\pi^-$, $\pi^+\pi^+\pi^-\pi^-$, and $B_s \rightarrow D_s\pi$, D_sK . Taking branching ratios into account, a single-lepton trigger (e.g., triggering on $\bar{B} \rightarrow l$ and then searching for associated B decay to hadrons) would not be a viable way to get adequate statistics. Instead, a silicon-based trigger on secondary vertices, coupled with trigger-level tracking cuts, appears to be a good way to capture large numbers of hadronic B decays, and CDF plans to deploy a silicon vertex trigger in Run II. A key feature that makes this workable in the central region is the very small transverse spread of the beam at the interaction point (IP). In Run I the typical beam spot size was ± 22 microns in both transverse dimensions. Thus, it is not necessary to reconstruct the primary vertex event by event in the trigger, but only to find tracks with large projected impact parameter with respect to the IP. For forward detectors (LHC-B and BTeV), the task will be more challenging because of the longitudinal spread of the interaction region.

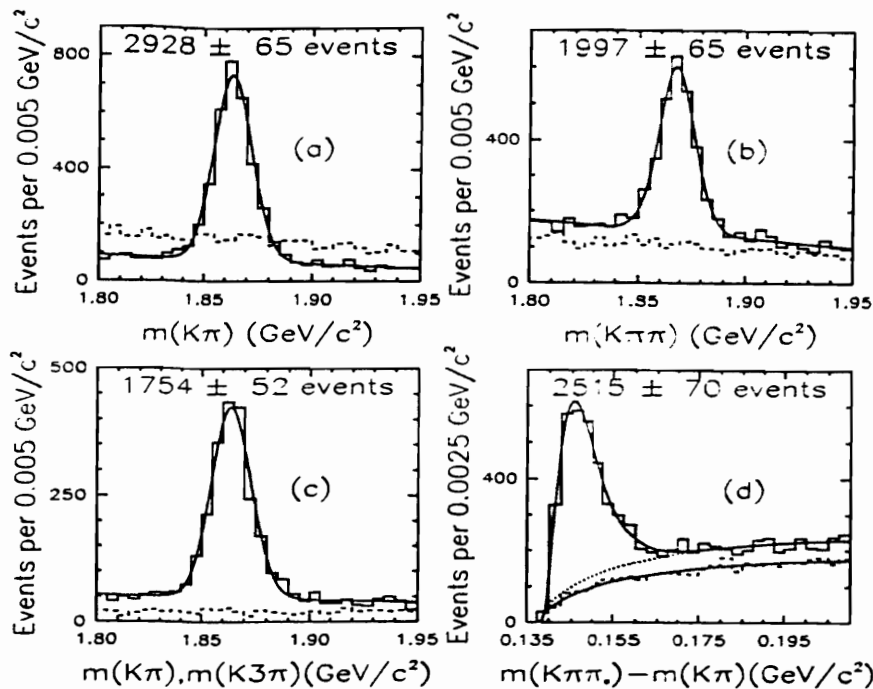


FIGURE 2. (Left) Charm peaks in $B^+ \rightarrow l^+ \nu \overline{D^0} X$ and $B^0 \rightarrow l^+ \nu D^{(*)-} X$: (a) $\overline{D^0} \rightarrow K^+ \pi^-$; (b) $D^- \rightarrow K^+ \pi^- \pi^-$; (c) $D^{*-} \rightarrow \overline{D^0} \pi^-$, $\overline{D^0} \rightarrow K^+ \pi^-$ or $K^+ \pi^+ \pi^- \pi^-$; (d) $D^{*-} \rightarrow \overline{D^0} \pi^-$, $\overline{D^0} \rightarrow K^+ \pi^- \pi^0$.

Below, we summarize physics topics that CDF has examined, including b production, spectroscopy, rare decays, lifetimes, and mixing properties. We then conclude with a brief overview of future plans.

CDF B PHYSICS RESULTS

Run 0

The CDF detector, as configured at the start of Run 0, is described in Ref. [7]. The most relevant components for B physics are the 3-meter-diameter by 3-meter-long central drift chamber, which covered the region $|\eta| \leq 1.2$; the central calorimeter, which featured fine-grained electromagnetic shower detection; and muon chambers located outside the central calorimeter at $5\lambda_{abs}$.

The first physics run in 1988–89 yielded samples of about 1000 $J/\psi + \psi'$, 40,000 inclusive leptons, and 900 $e\mu$ dilepton pairs. The $e\mu$ sample produced the first CDF publication on b physics, a measurement of $\overline{\chi}$, the species- and time-averaged mixing parameter [8].

Clear signals were seen for exclusive B hadron production in the modes $B^+ \rightarrow \psi K^+$ [9], $B^0 \rightarrow \psi K^{*0}$ [10], and $B \rightarrow e^+ \nu D^0$ [11]. These had a major impact on CDF's planning for B physics in Run I. The observed signals

corresponded to a substantially larger B hadron cross section than predicted by NLO QCD [12]. Likewise, the b quark inclusive cross sections, as determined with inclusive electron [11], muon [13], J/ψ , and ψ' [14] samples, also indicated higher than expected cross sections. In order to extract the b cross section from the charmonium samples, it was assumed that B 's were the main source of ψ' production and that B 's and $\chi_c \rightarrow \psi\gamma$ were the main sources of J/ψ production. It proved possible to measure the χ_c contribution, using the excellent CDF calorimeter segmentation to identify the soft photon in χ_c decay [15,16], and thus, by subtraction, infer the $b \rightarrow J/\psi$ contribution. With the assumption that *direct* J/ψ production is negligible, this measurement implied that $\sim 60\%$ of J/ψ 's originate from B decay. The high cross section was good news from an engineering standpoint (*i.e.*, better for a future b physics program), but seemed inconsistent with the older UA1 results at $\sqrt{s}=630$ GeV [17], and generated considerable interest in the theory community [18].

Run I

During 1989–1992 major improvements were made to both the Tevatron Collider and the CDF detector. The most important CDF upgrade component was the four-layer silicon vertex detector (SVX), located very close (3 to 8 cm radii) to the IP, yielding typical impact parameter resolutions of $13 + 40/p_T$ μm [3]. This device quickly resolved the cross section issues raised in Run 0. The SVX data allowed model-independent separation of B production in $B \rightarrow J/\psi, \psi', e\nu X, \mu\nu X\dots$ from backgrounds such as prompt charmonium production, $c\bar{c}$, and misidentified leptons. In particular, it was easy to show that a relatively small fraction ($\sim 20\%$) of J/ψ and ψ' production comes from B decay [19]. Also, the fraction of inclusive leptons coming from B decays was somewhat overestimated in the Run 0 analyses; the SVX measurements allowed precise determinations of the sample composition, including fake rates. The unexpectedly large cross sections for *direct* ψ and ψ' production are very interesting in their own right [20], but remain a background in the B physics industry.

Currently all Run I CDF B cross section measurements are based either on the SVX impact parameter data [21–23] or exclusive reconstruction [24,25]. Figure 3 shows examples of the exclusive and inclusive cross section measurements, compared with NLO QCD, using MRSD0 structure functions. Both the single b quark and B hadron, and the correlated $b\bar{b}$ cross sections in the central region are consistently 2–3 times higher than the nominal QCD predictions. To check the earlier discrepancy with UA1 data, CDF interleaved data at $\sqrt{s}=0.63$ TeV with $\sqrt{s}=1.8$ TeV at the end of Run I; this permitted a direct comparison of the b cross sections at the two energies with the same apparatus, the same decay channels (inclusive muons), and minimal systematic bias. The *ratio* of experimental cross sections at the two energies agrees well with

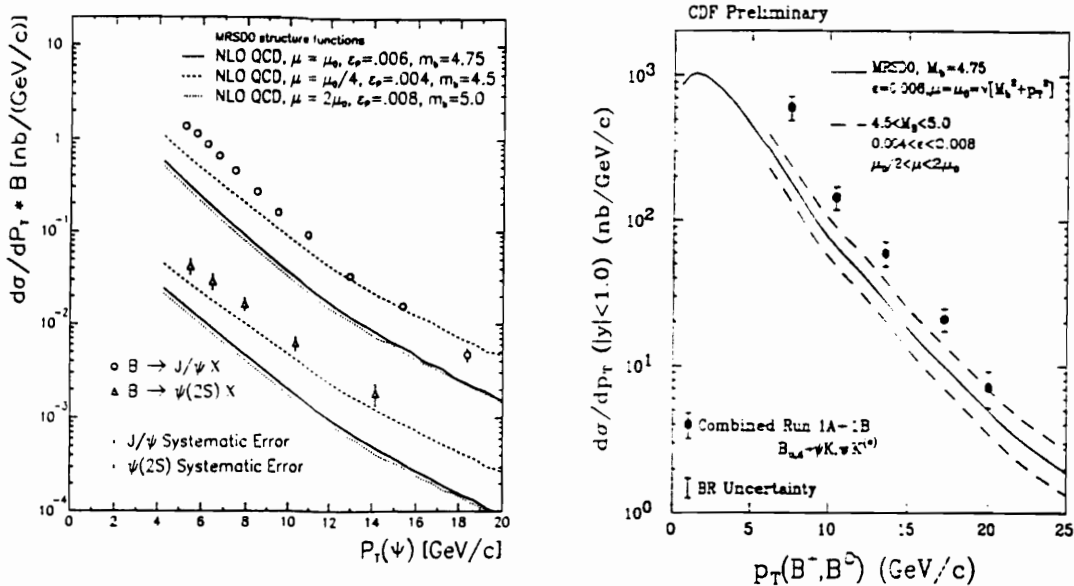


FIGURE 3. (left) Inclusive J/ψ and ψ' cross sections from B decay, compared with NLO QCD; (right) B^+ , B^0 differential cross sections compared with NLO QCD.

NLO QCD expectations [26]; however, the absolute cross sections (including UA1's) are systematically higher than the QCD predictions at both energies [27]. Thus, CDF cross section measurements show that the absolute yields and also the probability of finding the second b jet for tagging are favorable for a b physics program in the central region.

In addition to the SVX detector, other improvements to CDF augmented the b physics capability in Run I. First, the trigger strategies were optimized, using the experience gained in Run 0. By lowering thresholds, tightening trigger-matching cuts, and extending the muon coverage in η , CDF increased the yield of J/ψ 's per pb^{-1} from ~ 230 in Run 0 to ~ 4500 in Run I. The purity of the single muon triggers was improved using additional absorber with read-out chambers at $8\lambda_{abs}$; this reduced hadron punch-through backgrounds by a factor of twenty. The inclusive electron trigger purity was improved by matching the shower-maximum detector signal to the electron track [28]. Electron identification was also improved by addition of preshower detectors at $1X_0$. Relativistic rise dE/dx information was obtained from the outer 54 layers of the central drift chamber; with $\sim 9\%$ resolution, this gave $\sim 2\sigma$ separation between electrons and minimum ionizing particles, and allowed statistical separation of π^\pm , K^\pm , and p, \bar{p} . For slow particles, $\frac{1}{\beta^2} dE/dx$ was available from both the drift chamber and the SVX. Finally, it should be noted that the SVX provides not only precise impact parameter information; by matching tracks to secondary vertices, the SVX also allows clean reconstruction of multiparticle charm and bottom decays, such as $D^0 \rightarrow K^- \pi^+ \pi^- \pi^+$, which would be otherwise buried in combinatorial background. Overall, the CDF detector im-

provements in Run I allowed much larger bandwidths for single and dilepton triggers and better B purity than in Run 0.

Properties of b Hadrons

Masses

The exclusive J/ψ decay modes provide very straightforward signatures to measure b hadron masses. The J/ψ and ψ' decays themselves provide a built-in calibration for tracking systematics. With samples of 32 $B_s \rightarrow \psi\phi$ and 20 $\Lambda_b \rightarrow \psi\Lambda$ events, CDF measurements dominate the world averages for B_s [29] and Λ_b masses [30]. With much higher statistics in Run II, we can look forward to precision mass measurements for a variety of states using the J/ψ sample: B_s , Λ_b , Σ_b , Ξ_b , B_c , and strong-decay excitations (B^{**} , Σ_b^* , Λ_b^*).

Branching Ratios and Decay Distributions

CDF has used the exclusive J/ψ sample to establish relative branching ratios for the decays $B^+ \rightarrow \psi K^+$, $\psi' K^+$, ψK^{*0} , $B^0 \rightarrow \psi K^{*0}$, $\psi' K^{*0}$, ψK^0 , and $B_s \rightarrow \psi\phi$ [31-33], as well as the Cabibbo-suppressed decay $B^+ \rightarrow \psi\pi^+$ [34]. The decay angular distributions are used to study the CP -composition in $B_s \rightarrow \psi\phi$ and $B^0 \rightarrow \psi K^{*0}$ [35]; this information is potentially important for CP violation studies with these modes. The published CDF results on the longitudinal polarization fraction in $B^0 \rightarrow \psi K^{*0}$ are compatible with the recent CLEO analysis: $\Gamma_L/\Gamma = 0.65 \pm 0.10 \pm 0.04$ (CDF), $0.52 \pm 0.07 \pm 0.04$ (CLEO) [6]. A value $\Gamma_L/\Gamma = 1$ would signal a pure CP -even final state; the observed value is consistent with an admixture of even and odd partial waves, and a full angular distribution analysis is needed to separate the CP -odd P wave from the CP -even S and D waves. The published CDF result on $B_s \rightarrow \psi\phi$, $\Gamma_L/\Gamma = 0.56 \pm 0.21_{-0.04}^{+0.02}$, is also consistent with an admixture of even and odd waves. The current CDF results are based on 19 pb^{-1} , and with the full statistics of Run I and eventually Run II, it will be possible to carry out a precise determination of the full angular distribution for both ψK^{*0} and $\psi\phi$ modes, similar to the CLEO analysis on $B^0 \rightarrow \psi K^{*0}$ [6].

Rare Decays

CDF has set competitive limits on rare decays involving non-resonant dilepton final states, $B^+ \rightarrow K^+ \mu^+ \mu^-$ and $B^0 \rightarrow K^{*0} \mu^+ \mu^-$, as well as $B^0 \rightarrow \mu^+ \mu^-$ and $B_s \rightarrow \mu^+ \mu^-$ [36]. The limits on the first two modes are currently only an order of magnitude above the standard model expectations; CDF should have large enough dimuon samples in Run II to observe of order 100 or more

events in the $K^+\mu^+\mu^-$ and $K^0\mu^+\mu^-$ modes in Run II. These decays involve loop diagrams and are potentially sensitive to physics beyond the standard model.

Radiative Decays

CDF has also done a feasibility study on rare radiative decays. The relative branching ratios for $B^0 \rightarrow \rho\gamma$ to $B^0 \rightarrow K^{*0}\gamma$ or $B_s \rightarrow K^{*0}\gamma$ to $B_s \rightarrow \phi\gamma$ are proportional to the ratio of CKM matrix elements V_{td}^2/V_{ts}^2 , up to hadronic corrections of order unity. CDF implemented a photon-plus-two-charged-particle trigger for about 23 pb^{-1} integrated luminosity in Run I. Using standard photon identification and isolation cuts, and impact parameter cuts on the charged particles, the preliminary CDF analysis finds 1(0) signal candidate events with expected physics signals of 0.95 ± 0.51 (0.34 ± 0.18) events in the $K^{*0}\gamma$ ($\phi\gamma$) channels. Preliminary limits on the $B_s \rightarrow \phi\gamma$ decay branching ratio are found to be 3.9×10^{-4} at 90% confidence; so far, the only published limit on this mode is 7.0×10^{-4} from DELPHI [37]. A second experimental method is to use photon conversions into e^+e^- pairs in place of the photon in these final states. This would improve the mass resolution and the background rejection, using an electron rather than a photon trigger. The conversion radiator is supplied by the CDF inner detector (about 12% X_0 in Run II). Combining the conversion efficiency with the product branching ratios, the radiative decay signal, $B^0 \rightarrow K^{*0}\gamma$, would be around 3% of the "known" signal $B^0 \rightarrow K^{*0}\psi, \psi \rightarrow e^+e^-$, for which CDF expects several 1000's in Run II. CDF already has clean B peaks using $J/\psi \rightarrow e^+e^-$, and has shown the utility of conversion photons with cleanly resolved peaks in $\chi_c \rightarrow \psi\gamma$ [30].

Search for the B_c

The spectroscopy of $\bar{b}c$ states can best be studied at hadron colliders. The mass of the weakly decaying B_c is predicted to be 6.24–6.31 GeV [38], and its production rate is predicted to be around 4×10^{-3} relative to the B^+ meson [39]. The decay rate is expected to be the sum of \bar{b} and c decays plus the $\bar{b}c$ annihilation process; one of the more interesting experimental questions is whether the \bar{b} or c -quark decays first. Predictions for the lifetime range from 0.4 to 1.4 ps, depending on whether the decay is c or \bar{b} dominated [40]. Predictions are given in Ref. [41] for branching ratios into states involving J/ψ . Combining the theoretical assumptions, we get the following estimates for ratios of B_c to B^+ production:

$$\frac{B_c \rightarrow \psi l^+ \nu}{B^+ \rightarrow \psi K^+} \simeq 0.09 \times \frac{\tau}{0.5 \text{ ps}} \times \epsilon \quad (1)$$

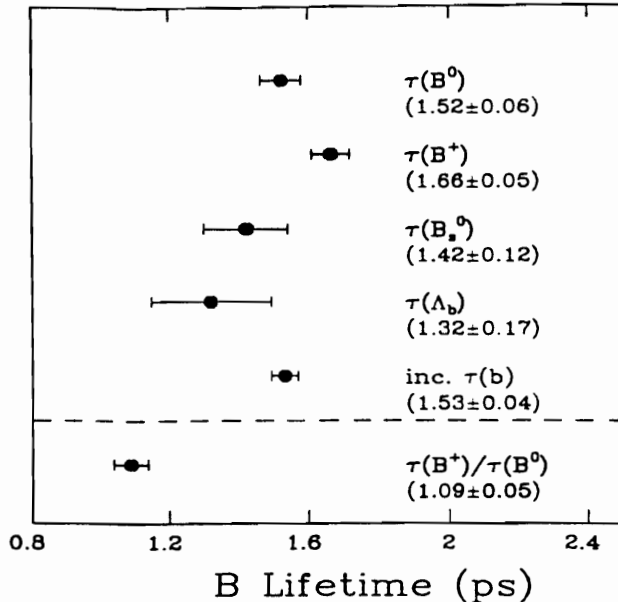


FIGURE 4. Exclusive B hadron lifetimes measured in CDF, combining J/ψ , ψ' and semileptonic modes. Also shown are the B^+/B^0 lifetime ratio and the species-averaged lifetime, the latter based on inclusive J/ψ and ψ' production. Values shown for B^+ , B^0 , and B_s are preliminary.

$$\frac{B_c \rightarrow \psi\pi^+}{B^+ \rightarrow \psi K^+} \simeq 0.009 \times \frac{\tau}{0.5ps} \times \epsilon, \quad (2)$$

where τ is the B_c lifetime and ϵ is the relative detection efficiency. CDF has published limits on the $\psi\pi^+$ mode [34], and has candidates in the semileptonic modes. The important point here is that CDF has a *large* $B^+ \rightarrow \psi K^+$ signal in the denominator (*c.f.*, Figure 1), and so the B_c signal should be detectable, depending on $\tau(B_c)$. ALEPH has reported a clean candidate event in the $\psi\mu^+\nu_\mu$ final state [42]; as noted earlier, the total yield of B hadron decays to J/ψ 's at LEP is substantially lower than the Run I CDF yields. Stay tuned!

Lifetime Measurements

In 1990 the PDG species-averaged lifetime for B hadrons was 1.18 ± 0.11 ps. The current average values are 1.538 ± 0.019 ps from LEP semileptonic decays and 1.533 ± 0.036 ps from CDF inclusive J/ψ decays. This underscores the dramatic impact that CDF, SLD, and LEP experiments have had on time-dependent measurements such as B lifetimes and mixing parameters. Current world averages on the individual B hadron lifetimes now approach accuracies of around 5%. The effects of non-spectator contributions have been calculated

with the heavy quark expansion technique [43,44]. The expected pattern for $\tau(\Lambda_b) : \tau B_s : \tau B^0 : \tau B^+$, $\sim 0.9:1.0:1.0:\sim 1.05$ appears to match the data fairly well, $0.79:0.98:1.00:1.06$ [45], although the short Λ_b lifetime is not understood.

CDF has measured the species lifetimes using large samples of semileptonic and exclusive J/ψ decays [46–52]. The systematic uncertainties are larger for the semileptonic samples, since the B hadron is not fully reconstructed (missing neutrino) and there are uncertainties associated with feeddown from excited charm states (e.g., D^{**} 's). For the exclusive J/ψ modes, typical systematic uncertainties are on the order of 1%, mainly due to modeling of the $c\tau$ resolution function. Since the semileptonic channels have higher statistics, the errors are comparable for both modes, but it is likely that after Run II all of the B hadron lifetimes, like the mass measurements, will be dominated by the J/ψ data. Figure 4 shows a summary of the CDF results with semileptonic and J/ψ modes combined. The values are in good agreement with the LEP results and the world averages [45].

Two additional lifetime measurements are accessible at hadron colliders, namely the B_c lifetime discussed above and the lifetime difference between the short and long-lived B_s states (expected to be the predominantly CP -even and odd $B_s \pm \bar{B}_s$ mixing eigenstates, respectively). Theoretical estimates give $\Delta\Gamma/\Gamma \sim 0.16$ [53,54], with phenomenological upper limits, based on $b \rightarrow c\bar{c}s$ transition rates, of $\Delta\Gamma/\Gamma \leq 0.44 \pm 0.06$ [53]. With the present sample of 420 $B_s \rightarrow l\nu D_s X$ events, CDF has probed the sensitivity of a double exponential fit to separate the two lifetimes; extrapolating from this, CDF should be able to measure $\Delta\Gamma/\Gamma$ to ± 0.02 – 0.03 in Run II. If $\Delta\Gamma/\Gamma$ is indeed large, it would open up new avenues to CP violation, including the elusive phase γ [53]. In the limit of large $\Delta\Gamma/\Gamma$, the B_s system would be similar to the $K_L - K_S$ system; the separability of the two eigenstates by lifetime acts like a flavor tag, and allows one to compare the CP properties in the decay of each eigenstate. In addition, if the difference is large, the relation between ΔM and $\Delta\Gamma$ can be used to estimate x_s for the B_s [53].

Time-Dependent Mixing

Time-dependent measurements of $B^0\bar{B}^0$ oscillations at LEP, SLD, and CDF have yielded precise values for the mass difference, $|\Delta m_d|$, between the neutral B_d eigenstates. Eventually, combined with accurate measurements of the mass difference for the B_s eigenstates, this information should lead to relatively model-independent determinations of $|V_{td}|/|V_{ts}|$.

The current CDF analyses of B_d -mixing are based on semileptonic decays, using both the high- p_T single lepton and lower- p_T dilepton trigger samples. In all cases, one of the leptons is combined with other charged particles in the same b jet to measure the decay vertex in the transverse plane and to estimate $\beta\gamma$ and the proper decay time. The analyses further split depending

on whether the charged particles accompanying the lepton are reconstructed as charmed D^0 , D^+ , and D^{*+} or are treated inclusively. In both cases, the B hadron flavor at decay time is tagged by the decay lepton. In the reconstructed charm sample, illustrated in Figure 2, the B_d^0 is identified by its semileptonic decay (with a few % cross-talk from charged B decays). In the inclusive samples, the B_d^0 time-dependent oscillation must be extracted from backgrounds from B^+ , B_s , and Λ_b decays.

The flavor of the B hadron at birth is deduced either from the associated “away-side” b jet or from the fragmentation products in the “same-side” \bar{b} -jet. For the dilepton trigger samples, the away-side jet is tagged using the second trigger lepton. For the inclusive single lepton triggers, both away-side tags, based on soft leptons or jet charge, and same-side (SST) tags, based on the fragmentation charge, are used.

To date, these combinations have led to five CDF measurements of Δm_d , which are shown in Figure 5. These are:

- (1) single lepton-plus-charm with SST ($\sim 9\text{K}$ events- *c.f.*, Figure 2)
- (2) single inclusive lepton with away-side tag on soft lepton or jet charge ($\sim 250\text{K}$ events)
- (3,4) inclusive lepton from both $e\mu$ and $\mu\mu$ dilepton samples ($\sim 20\text{K}$ events)
- (5) lepton-plus-charm from dilepton sample ($\sim 0.5\text{K}$ events)

The lepton-plus-charm samples are essentially pure B , after sideband subtraction on the mass peaks. The inclusive lepton samples are also very pure in B content, after selecting lepton plus charged particle jets having displaced vertices; the b fractions are estimated using the lifetime distributions, the jet mass, and the lepton $p_T(\text{rel})$, and are typically of order 90%.

The time-dependent oscillation is given by

$$B_{\text{tag}}^0(0) \rightarrow B^0(t) = \frac{e^{-\Gamma t}}{2} [1 + D \cos \Delta m t] \quad (3)$$

$$B_{\text{tag}}^0(0) \rightarrow \bar{B}^0(t) = \frac{e^{-\Gamma t}}{2} [1 - D \cos \Delta m t]; \quad (4)$$

the equations give the relative probabilities for a neutral B , tagged as a B^0 at birth ($t = 0$) to decay as a B^0 or a \bar{B}^0 at time t ; Δm is the oscillation frequency; and D is the flavor tagging “dilution” ($D = 2R - 1$, where R is the probability for a right-sign tag). The known variation of D as a function of the event variables (for example, $p_T(\text{rel})$ for lepton tags, or charge sum for jet-charge tags) is input to the maximum likelihood fits for each event. The fits then determine the overall magnitude of D from the amplitude of the mixing oscillation and Δm_d from the phase.

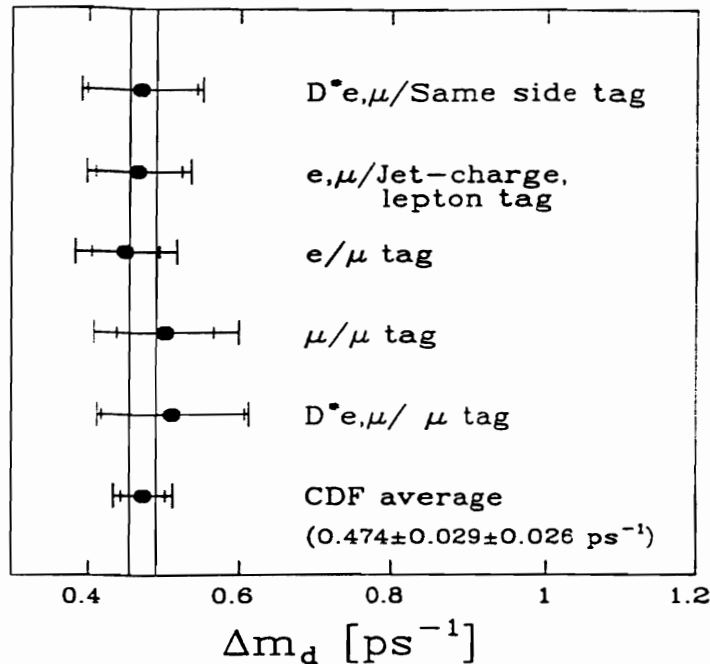


FIGURE 5. Summary of CDF measurements (preliminary) of Δm_d in the $B^0 - \overline{B}^0$ system. The band shows the current world average from LEP, SLD, and CDF measurements. The labels give the B_d decay signature/ tagging method.

If we denote the overall tagging efficiency, including right- and wrong-sign tags, as ϵ , then the statistical accuracy of a sample of N signal events corresponds to that of a tagged sample of size $N \times \epsilon D^2$. From the inclusive lepton analyses, the figure of merit for the different tagging methods, ϵD^2 , is found to be:

$$\epsilon D^2 \simeq 0.8\% \text{ (away-side jet charge)}$$

$$\epsilon D^2 \simeq 1.1\% \text{ (away-side lepton tags)}$$

$$\epsilon D^2 \simeq 2.4\% \text{ (SST on } B^0\text{)}$$

$$\epsilon D^2 \simeq 5.2\% \text{ (SST on } B^+\text{)}$$

The away-side tagging methods (jet-charge and lepton tags) are handicapped by several effects: mixing of the away side jet, which gives an intrinsic $D_{\text{mix}} = 1 - 2\overline{\chi}$; sequential decays for leptons; the limited η coverage of the present CDF tracking system; and background tags from gluon jets at small η . The same-side tags do not suffer from these effects and so yield a higher efficiency. In the CDF SST algorithm, prompt tracks from the $b \rightarrow B$ fragmentation or from B^{**} decay [55] are selected, and the parent B hadrons are tagged according to the expected correlations: $B^0\pi^+$, $\overline{B}^0\pi^-$, $B^+\pi^-$, and $B^-\pi^+$. As an example, Figure 6 shows the time dependence of the $B \rightarrow \overline{B}$ transition using SST tags;

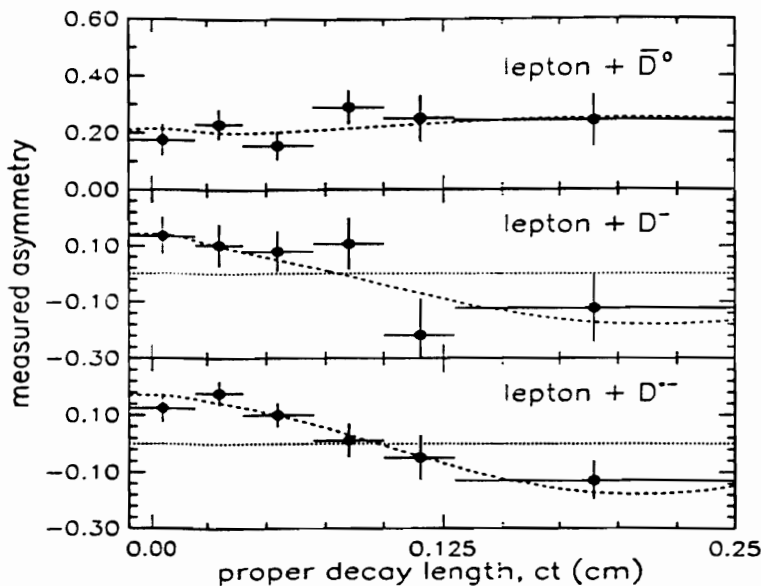


FIGURE 6. Measured asymmetry, $(B_{tag}(0) \rightarrow B) - (B_{tag}(0) \rightarrow \bar{B})$ for charged (top) and neutral B 's (middle and bottom). The curves show the mixing fits; the amplitudes are given by the SST dilution factors.

neutral B 's show the expected mixing oscillation, while charged B 's, used as a check on the method, do not [56].

THE FUTURE

With the main injector, the Tevatron is expected to deliver luminosities of order 2×10^{32} , and both the CDF and D0 experiments expect an integrated luminosity of 2 fb^{-1} in Run II. To handle the higher luminosities and shorter (396 ns) bunch spacing, the CDF detector is undergoing a major renovation [4]. The silicon vertex-tracking system will be upgraded from the present single-sided 4-layer device to a double-sided 7-layer system having both $X - Y$ and $R - Z$ readout; the new device will cover 90% of the luminous region in Z , compared with $\sim 60\%$ in the Run I device, and will be capable of standalone track reconstruction to $\eta=2$. These features should improve the signal-to-noise for B reconstruction and will increase the tagging efficiency for all tagging methods. In addition, the central drift chamber will be replaced, and high- p_T tracks ($p_T \geq 1.5 \text{ GeV}/c$) will be available for the level-1 decision. The trigger itself will be pipelined to accommodate a 50 kHz rate out of level-1; this bandwidth requirement is driven primarily by the all-hadronic B trigger. At the second trigger level, drift-chamber tracks

found in level-1 will be matched to the silicon vertex-detector hits, allowing offline-quality information on the track impact parameters. Fast processors in level-2 can then be used to form track-based triggers with secondary-vertex cuts, as well as the traditional lepton-based triggers. The third level trigger, which will perform event reconstruction using the full event readout, will select inclusive lepton, dilepton, and J/ψ samples as in Run I, and also the all-hadronic triggers needed for studies of CP violation ($B^0 \rightarrow \pi^+\pi^-$) and B_s mixing ($B_s \rightarrow D_s^- \pi^+, D_s^- \pi^+ \pi^+ \pi^-$.)

We have already alluded to some of the B physics goals that can be met with very high statistics lepton and J/ψ samples in Run II, for example:

- Precision masses and lifetimes for fully reconstructed B 's
- Determination of $\frac{\Delta\Gamma}{\Gamma}$ for B_s , using $B_s \rightarrow l^+ \nu D_s^-, \psi\phi$
- Observation of rare decays, $B^+ \rightarrow \mu^+ \mu^- K^+, B^0 \rightarrow \mu^+ \mu^- K^{*0}$
- Radiative decay branching ratios, e.g., $B_s \rightarrow \phi\gamma, B_s \rightarrow K^{*0}\gamma$
- Detailed studies of the B_c meson

In addition, CDF expects to:

- Observe CP violation in the channels $B_d^0 \rightarrow \psi K_s^0$ and $B_d^0 \rightarrow \pi^+\pi^-$
- Search for CP violation in $B_s^0 \rightarrow \psi\phi$ ($=0$ in S.M.)
- establish $\Delta m(B_s)$ using all-hadronic B_s triggers.

CP Violation

We conclude with a brief discussion of CP violation studies in Run II. The general form for the time evolution for B^0 decays to CP -eigenstates like ψK_s^0 and $\pi^+\pi^-$ is given by

$$a_{CP}(B_d \rightarrow f; t) = A_{CP}^{dir} \cos \Delta(m_d t) + A_{CP}^{mix} \sin \Delta(m_d t), \quad (5)$$

where the CP -violating asymmetry is defined by

$$a_{CP}(B_d \rightarrow f; t) = \frac{(B_d^0(t) \rightarrow f) - (\overline{B_d^0(t)} \rightarrow f)}{(B_d^0(t) \rightarrow f) + (\overline{B_d^0(t)} \rightarrow f)}. \quad (6)$$

Here, " $B_d^0(t) \rightarrow f$ " is the probability for a neutral B , produced as a B^0 at $t = 0$, to decay to the CP -eigenstate f at time t ; A_{CP}^{dir} denotes direct CP violation in the decay, while A_{CP}^{mix} denotes CP violation due to interference between mixing and decay processes [57]. For the final state $f = \psi K_s$, the first term in Eq. (5) is expected to be small, and the mixing induced term A_{CP}^{mix} is given by the quantity $-\sin(2\beta)$. For the final state $f = \pi^+\pi^-$, the first

term could be large, depending on penguin contributions; the mixing induced term A_{CP}^{mix} is given by $-\sin(2\alpha)$ plus possible additional contributions from penguin amplitudes.

As with mixing measurements, the observed asymmetry is reduced by the tagging dilution factor D :

$$a_{CP}^{obs.} = D \times a_{CP}(B_d \rightarrow f; t) \quad (7)$$

Thus, it is necessary to calibrate the dilution accurately. For the away-side tagging methods, D can be calibrated directly using the high-statistics sample of $B^+ \rightarrow \psi K^+$ [58]. For “same side tagging”, since B^+ and B^0 have different charge correlations with the fragmentation tracks, D must be calibrated using the mixing oscillation signal from $B_d^0 \rightarrow \psi K^{-0}$, supplemented by mixing measurements using B_d^0 semileptonic decays.

Extrapolating from the observed event yields in Run I, taking into account lower trigger thresholds and better tagging coverage with the upgraded detector, CDF expects to obtain up to 15,000 ψK_S events in Run II (2fb^{-1}), with overall tagging efficiency $\sim 5.4\%$ [4]. A simple time-averaged asymmetry measurement would yield an uncertainty

$$\delta \sin(2\beta) \simeq \frac{1 + x_d^2}{x_d} \frac{1}{\sqrt{\epsilon D^2 N}} \sqrt{\frac{S + B}{B}}, \quad (8)$$

where the dilution factor $(1 + x_d^2)/x_d = 2.13$ arises from time averaging the $\sin \Delta m_d t$ dependence, and S/B is the signal to background. With these input assumptions, $\delta \sin(2\beta) = 0.09$. In practice, it will be necessary to fit the time dependence. This verifies the $\sin(\Delta m_d t)$ dependence expected for A_{CP}^{mix} and reduces $\delta \sin(2\beta)$; it also improves the effective signal to background, since the combinatorial background from prompt J/ψ production occurs at $t = 0$, where the CP asymmetry should vanish.

Assuming a nominal $BR(B_d^0 \rightarrow \pi^+\pi^-)$ of 1×10^{-5} , the all-hadronic trigger designed for CDF in Run II would yield approximately 10,000 events in this mode [4]. Ignoring A_{CP}^{dir} , Monte Carlo studies indicate that an error $\delta \sin(2\alpha) \sim 0.12$ can be achieved, with the same ϵD^2 as for ψK_S above. Again, it will be necessary to fit the time dependence, and here the penguin-induced $\cos(\Delta m_d t)$ oscillations may turn out to be large. In that case, the interpretation of “ $\sin(2\alpha)$ ” is more complicated; some strategies for this case are discussed in Ref. [59]. In addition to the possible complications from penguin diagrams, backgrounds are expected from $B_d^0 \rightarrow K^+\pi^-$ and $B_s^0 \rightarrow K^-\pi^-, K^-K^-$, which overlap the $\pi^+\pi^-$ mass distribution within $\sim \pm 2\sigma$. Neither of these backgrounds would contribute to the $\sin(\Delta m_d t)$ oscillation, but they introduce an overall dilution factor in the observed asymmetry [60]. This overall dilution can be determined by measuring the total background from $K^+\pi^-$ and K^+K^- production using relativistic-rise dE/dx measurements from the

central drift chamber; this purely statistical separation can be done on the full signal sample before tagging. Since the time-dependence of the CP asymmetry is especially important for $B_d^0 \rightarrow \pi^+\pi^-$, it is worth noting that the proper time resolution is quite good in this mode due to the large opening angle between the decay pions. With the all-hadronic trigger selections and just the Run I silicon vertex resolution, the average resolution on the decay proper time would be around 6% of the B_d^0 lifetime; this should improve with 3D vertexing in Run II.

CONCLUSION

CDF has shown that it is possible to take advantage of the high B hadron production rates in the central region at the Tevatron, using selected triggers. The very high yields and the mix of B hadron flavors make the hadron-collider B program complementary to that at e^+e^- B factories. With the upgraded CDF detector, it should be possible to increase the present samples of J/ψ and lepton triggers by factors of fifty. CDF also plans to deploy all hadronic silicon-based triggers for studies of CP violation and B_s mixing. Thus, the CDF collaboration is optimistic that after ten years of experience doing B physics at the Tevatron, the best is still yet to come.

REFERENCES

1. D. Ayres et al., *Design Report for the Fermilab Collider Detector Facility*, 1981 (unpublished).
2. There was, nevertheless, appreciation of the potential for b physics at hadron colliders. See for example: R. Diebold and J. Sauer, *Electron Identification in Jets*, CDF Note 72 (1980); L. L. Chau et al., *Heavy Quark Jets*, Proc. 1982 Summer Study on Elementary Particle Physics and Future Facilities, Snowmass (1982), p. 510.
3. D. Amidei et al., *Nucl. Instrum. Methods A* **269**, 93 (1988).
4. The CDF II Collaboration, *The CDF II Detector Technical Design Report*, FERMLAB-Pub-96/390-E.
5. OPAL Collaboration, *Z. Phys.* **C70**, 197 (1996).
6. CLEO Collaboration, *Measurement of the Decay Amplitudes and Branching Fractions of $B \rightarrow J/\psi K^{*0}$ and $B \rightarrow J/\psi K$ Decays*, CLNS 96/1455.
7. CDF Collaboration, F. Abe et al., *Nucl. Instrum. Methods Phys. Res. Sect. A* **271**, 387 (1988).
8. CDF Collaboration, F. Abe et al., *Phys. Rev. Lett.* **67**, 3351 (1991).
9. CDF Collaboration, F. Abe et al., *Phys. Rev. Lett.* **68**, 3403 (1992).
10. CDF Collaboration, F. Abe et al., *Phys. Rev. D* **50**, 4252 (1994).
11. CDF Collaboration, F. Abe et al., *Phys. Rev. Lett.* **71**, 500 (1993).

12. P. Nason, S. Dawson, and R. K. Ellis, *Nucl. Phys.* **B303**, 607 (1988); *ibid* **327**, 49 (1989); *ibid* **B335**, 260 (1990).
13. CDF Collaboration, F. Abe *et al.*, *Phys. Rev. Lett.* **71**, 2396 (1993).
14. CDF Collaboration, F. Abe *et al.*, *Phys. Rev. Lett.* **69**, 3704 (1992).
15. CDF Collaboration, F. Abe *et al.*, *Phys. Rev. Lett.* **71**, 2537 (1993).
16. CDF Collaboration, F. Abe *et al.*, *Phys. Rev. Lett.* **79**, 578 (1997).
17. N. Ellis and A. Kerner, *Phys. Rep.* **195**, 23 (1990).
18. E. Berger, R. Meng, and W. K. Tung, *Phys. Rev. D* **46**, 1859 (1992); M.L. Mangano, *Z. Phys.* **C58**, 861 (1992); J. Smith and W. K. Tung, *Proceedings of the Workshop on B Physics at Hadron Accelerators* Snowmass, Co. (1993), P. McBride and C. S. Mishra, ed.
19. CDF Collaboration, F. Abe *et al.*, *Phys. Rev. Lett.* **71**, 3421 (1993).
20. R. K. Ellis, W. J. Stirling, and B. R. Webber, *QCD and Collider Physics*, Cambridge Univ. Press, 1996, ch. 10.
21. CDF Collaboration, F. Abe *et al.*, *Phys. Rev. D* **53**, 1051 (1996).
22. CDF Collaboration, F. Abe *et al.*, *Phys. Rev. D* **55**, 2546 (1997).
23. CDF Collaboration, F. Abe *et al.*, *Phys. Rev. Lett.* **79**, 572 (1997).
24. CDF Collaboration, F. Abe *et al.*, *Phys. Rev. Lett.* **75**, 1451 (1995).
25. The CDF Collaboration, *Measurement of the B-Meson Differential Cross-Section in $p\bar{p}$ Collisions at $\sqrt{s}=1.8$ TeV*, FERMILAB-CONF-96/198-E.
26. CDF Collaboration, *Measurement of the Ratio of b Quark Production Cross-Sections at $\sqrt{s}=630$ GeV and $\sqrt{s}=1800$ GeV*, FERMILAB-CONF-96/176-E.
27. To avoid confusion, note that the older cross section comparisons used DFLM structure functions in the NLO QCD predictions; more modern structure functions such as MRSD0 and MRSA predict significantly smaller b cross sections.
28. K. Byrum *et al.*, *Nucl. Instrum. Methods* **A364** 144 (1995).
29. CDF Collaboration, F. Abe *et al.*, *Phys. Rev. D* **53**, 3496 (1996).
30. CDF Collaboration, F. Abe *et al.*, *Phys. Rev. D* **55**, 1142 (1997).
31. CDF Collaboration, F. Abe *et al.*, *Phys. Rev. Lett.* **76**, 2015 (1996).
32. CDF Collaboration, F. Abe *et al.*, *Phys. Rev. D* **54**, 6596 (1996).
33. CDF Collaboration, *Branching Fractions of $B^+ \rightarrow \psi(2S)K^+$ and $B^0 \rightarrow \psi(2S)K^{*0}$ Decays at CDF*, FERMILAB-CONF-96/160-E.
34. CDF Collaboration, F. Abe *et al.*, *Phys. Rev. Lett.* **77**, 5176 (1996).
35. CDF Collaboration, F. Abe *et al.*, *Phys. Rev. Lett.* **75**, 3068 (1995).
36. CDF Collaboration, F. Abe *et al.*, *Phys. Rev. Lett.* **76**, 4675 (1996).
37. DELPHI Collaboration, *Z. Phys.* **C72**, 207 (1996).
38. E. Eichten and C. Quigg, *Phys. Rev. D* **49**, 5845 (1994); W. Kwong and J. Rosner, *Phys. Rev. D* **44**, 212 (1991).
39. E. Braaten, K. Cheung, and T. C. Yuan, *Phys. Rev. D* **49**, R5049 (1996).
40. M. Beneke and G. Buchala, *Phys. Rev. D* **53**, 4991 (1996); I. I. Bigi, *Phys. Lett.* **B371**, 105 (1996).
41. C. H. Chang and Y. Q. Chen, *Phys. Rev. D* **49**, 3399 (1994).
42. ALEPH Collaboration, *Search for the B_c meson in hadronic Z decays*, CERN-PPE/97-026.
43. M. B. Voloshin and M. A. Shifman, *Sov. Phys. JETP* **64**, 698 (1986); I. I. Bigi

- et al.*, *B Decays*, 2nd ed., S. Stone (ed.), World Scientific, Singapore (1994); I. I. Bigi, *UND-HEP-95-BIG02*; G. Bellini, I. I. Bigi, and P. J. Dornan, *Phys. Rep.* **289**, 1 (1997).
44. M. Neubert and C. T. Sachrajda, *Nucl. Phys. B* **483**, 339 (1997).
 45. T. R. Junk, *A Review of B Hadron Lifetime Measurements*, 2nd. Int. Conf. on B Physics and CP Violation, Honolulu (1997).
 46. CDF Collaboration, F. Abe *et al.*, *Phys. Rev. Lett.* **74**, 4988 (1995).
 47. CDF Collaboration, F. Abe *et al.*, *Phys. Rev. Lett.* **72**, 3456 (1994).
 48. CDF Collaboration, F. Abe *et al.*, *Phys. Rev. Lett.* **76**, 4462 (1996).
 49. CDF Collaboration, F. Abe *et al.*, *Phys. Rev. Lett.* **77**, 1439 (1996).
 50. CDF Collaboration, F. Abe *et al.*, *Phys. Rev. Lett.* **77**, 1945 (1996).
 51. CDF Collaboration, *B States and Lifetimes at CDF*, FERMILAB-CONF-96/155-E.
 52. CDF Collaboration, *Measurement of the Lifetime of the B_s Meson from $D_s^- l^+$ Correlations*, FERMILAB-CONF-96/154-E.
 53. M. Beneke, G. Buchalla, and I. Dunietz, *Phys. Rev. D* **54**, 4419 (1996).
 54. M. Voloshin, M. Shifman, N. Uraltsev, and V. Khoze, *Sov. J. Nucl. Phys.* **46**, 112 (1987).
 55. M. Gronau, A. Nippe, and J. Rosner, *Phys. Rev. D* **47**, 1988 (1993). In the present analysis, CDF does not distinguish B^{**} daughters from other fragmentation tracks.
 56. CDF Collaboration, *Observation of $\pi - B$ Charge-Flavor Correlations and Measurement of Time-Dependent $B^0 \bar{B}^0$ Mixing in $p\bar{p}$ Collisions*, FERMILAB-CONF-96/175-E.
 57. Y. Nir and H. Quinn, *Ann. Rev. Nucl. Part. Sci.* **42**, 211 (1992); A. Buras and R. Fleischer, *Quark Mixing, CP Violation and Rare Decays After the Top Quark Discovery*, in *Heavy Flavors II*, A. J. Buras and M. Lindner (ed.), World Scientific (1997); I. I. Bigi and A. I. Sanda, *Nucl. Phys. B* **281**, 41 (1987).
 58. This assumes that the away-side tagging dilution is the same for B^+ and B^0 hadrons. This is clearly not the case at the $\Upsilon(4S)$, where a B^+ hadron is tagged by an away-side B^- , while a B^0 hadron is tagged by an away-side \bar{B}^0 . At either a hadron collider or an $\Upsilon(4S)$ B factory, the time-averaged CP asymmetry for $B^0 \bar{B}^0$ states produced in odd- L waves vanishes due to Bose statistics. At the hadron collider, this is exactly compensated by the larger CP asymmetry in the even- L waves. So long as the $B^0 \bar{B}^0$ states are a stochastic mix of even- and odd- L states, the dilution measured with B^+ hadrons is the one needed in Eq. (7) for the B_d^0 CP -asymmetry.
 59. F. DeJongh and P. Sphicas, *Phys. Rev. D* **53**, 4930 (1996).
 60. The B_s contributions have much faster oscillations than the $\sin(\Delta m_d t)$ term. The $B_d^0 \rightarrow K^+ \pi^-$ backgrounds could contribute to the $\cos(\Delta m_d t)$ oscillation term if there is intrinsic CP violation leading to $B_d^0 \rightarrow K^+ \pi^- \neq \bar{B}_d^0 \rightarrow K^- \pi^+$.